

Statistical and Adaptive Signal Processing for UXO Discrimination for Next-generation Sensor Data

S. L. Tantum, Y.-Q. Wang, and L. M. Collins

Duke University, USA

Abstract—Until recently, detection algorithms could not reliably distinguish between buried UXO and clutter, leading to many false alarms. Over the last several years modern geophysical techniques have been developed that merge more sophisticated sensors, underlying physical models, statistical signal processing algorithms, and adaptive training techniques. These new approaches have dramatically reduced false alarm rates, although for the most part they have been applied to data collected at sites with relatively benign topology and anomaly densities. On more challenging sites, performance of even these more modern discrimination approaches is still quite poor. As a result, efforts are underway to develop a new generation of UXO sensors that will produce data streams of multi-axis vector or gradiometric measurements, for which optimal processing has not yet been carefully considered or developed. We describe a research program to address this processing gap, employing a synergistic use of advanced phenomenological modeling and signal-processing algorithms. The key foci of the program are (1) development of new physics-based signal processing approaches applicable to the problem in which vector data is available from such sensors; and (2) development of the theory of optimal experiments to guide the optimal design and deployment of the new sensor modalities. Here, we present initial results using simulated data obtained with our phenomenological models that indicate that optimal processing of features extracted from multi-axis EMI data can provide substantial improvements in discrimination performance over processing of features extracted from single-axis data.

1. Introduction

Until recently, detection algorithms have not reliably distinguished between buried UXO and clutter, leading to many false alarms. Over the last several years modern geophysical techniques have been developed that merge more sophisticated sensors, underlying physical models, statistical signal processing algorithms, and adaptive training techniques. These new approaches have significantly reduced false alarm rates, although for the most part they have been applied to data collected at sites with relatively benign topology and anomaly densities [1–5]. Most recently, blind source separation techniques have been applied to data collected on *highly cluttered* sites with commensurate reductions in the false alarm rates [6]. However, UXO clearance activities are ongoing or are planned at a wide variety of sites, and many of these activities involve complex terrain, vegetation and difficult geology, in addition to complex ordnance and clutter distributions. Moreover, most existing processing algorithms have been developed based on data associated with traditional sensors, such as CS-vapor magnetometers and coil-based electromagnetic induction sensors. Although these sensors are quite sensitive, they provide only limited information at any given survey point, as they do not illuminate the object under scrutiny along all three major axes. These limitations necessitate the use of high density spatial maps of anomalies, sometimes requiring multiple surveys, in order to collect data that support target localization and identification. Several investigators have noted that survey techniques that provide multi-angle illumination, while slower, improve discrimination performance [7, 8]. Others have shown theoretically or in limited field studies that sensors capable of multi-axis transmission provide data that result in improved object discrimination, as the parameters associated with the subsurface object are estimated more precisely [9].

In our previous efforts, we have successfully applied statistically-based signal processing algorithms using spatially-collected scalar EMI and magnetometer data for UXO discrimination. In one approach, probability density functions are developed that describe the statistical behavior of the data, x , obtained from a given sensor suite under the target and non-target hypotheses, denoted H_1 and H_0 , respectively. Given these probability density functions, $f(x|H_1)$ and $f(x|H_0)$, and a vector of sensor data, x , the optimal decision statistic, or likelihood ratio test (LRT), is utilized to make a decision regarding the appropriate hypothesis, this represented as $\Lambda(x) = f(x|H_1)/f(x|H_0)$. For EMI and/or magnetometer data, the vector x typically contains the parameters estimated from the data using a phenomenological model. (We discuss automatic feature selection algorithms below.) Features are estimated using a constrained search methodology. We have demonstrated that the multiple-local-minima problem associated with this search is largely mitigated using multi-axis sensor data,

thus resulting in better parameter estimates and better discrimination performance [9,10]. The probability density functions associated with the data under each hypothesis are estimated from training data.

Both the LRT and other approaches have been applied to several data sets, with outstanding results [2, 10]. Performance on several data sets indicated that these approaches performed very well when relevant training data were available. In particular, in one demonstration, these algorithms were scored in a blind test. Our goal in this current effort is to develop robust statistical signal processing techniques for data obtained from multi-axis sensors. Such processing has not previously been developed. We are considering simulated modeled on data from sensors already in development (e.g., Zonge nanoTEM system, the LBL/Morrison time-domain sensor, the USGS TMGS system, the QM MTG system, and the Oak Ridge SQUID-based system).

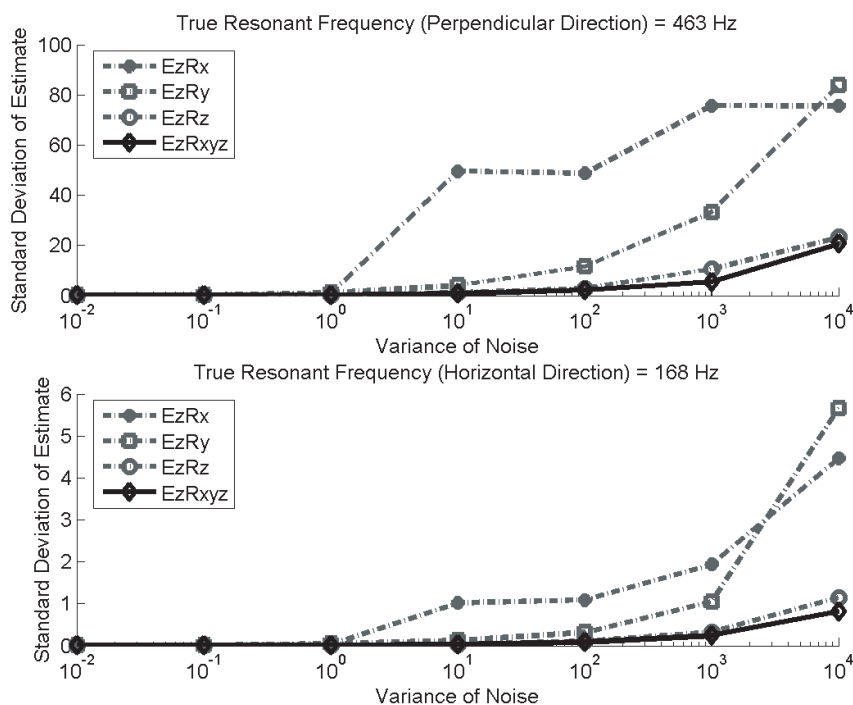


Figure 1: Standard deviation as a function noise variance for four different system configurations as noted in the legend. *Ez* indicates an excitation coil whose axis is perpendicular to the ground (*z* dimension), *Rx*, *Ry*, *Rz* denote receive coils in the *x*, *y*, and *z* dimension, and *Rxyz* denotes three receive coils, one in each of the dimensions.

2. Results

Typical electromagnetic induction (EMI) systems used for UXO detection had discrimination have two co-located coils—one used for transmitting the electromagnetic field, one used for receiving the field induced in the subsurface object. Historically, these coils have been located so that the axis of the coil is perpendicular to the ground. As noted above, recent studies have suggested that adding additional transmitter and/or receiver coils in different orientations can improve sensitivity and discrimination performance. The goal of this preliminary study was to assess the level of performance gain using simulated data, but realistic field scenarios and uncertainties.

It has been established that UXO can be adequately modeled using a dipole model [2, 4, 5, 8–10]. The imaginary resonant frequencies of the EMI resonant modes are a function of target material parameters. Thus, these features can be used after the data is inverted using the model for signal processing and classification. Imagine a cylinder coordinate system with the target's symmetry axis as *z*, the frequency-dependent moment can be expressed as

$$M(w) = \hat{z}\hat{z}[m_z(0) + \sum_k \frac{wm_{zk}}{w - jw_{zk}}] + (\hat{x}\hat{x} + \hat{y}\hat{y})[m_p(0) + \sum_i \frac{wm_{pi}}{w - jw_{pi}}]$$

The six target moment parameters are $m_z(0)$, $m_p(0)$, m_{zk} , m_{pi} , w_{zk} , and w_{pi} , where $m_z(0)$ and $m_p(0)$ account for the dipole moments contributed by ferrous targets. Parameters w_{zk} and w_{pi} are resonant frequencies, which are determined by the target geometry and material properties. Generally the first term in the sum, which is the principle dipole moment along each coordinate axis, is all that is needed to provide an accurate representation of the measured data from UXO and clutter.

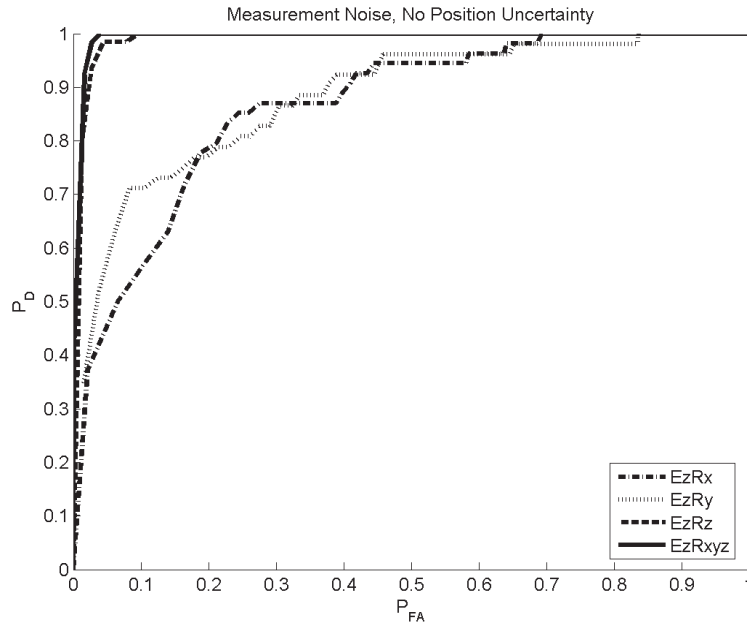


Figure 2: ROC curves plotting probability of detection versus probability of false alarm for the case where measurement noise is included, but it is assumed that measurement position is known perfectly. Single axis and multi-axis results are shown.

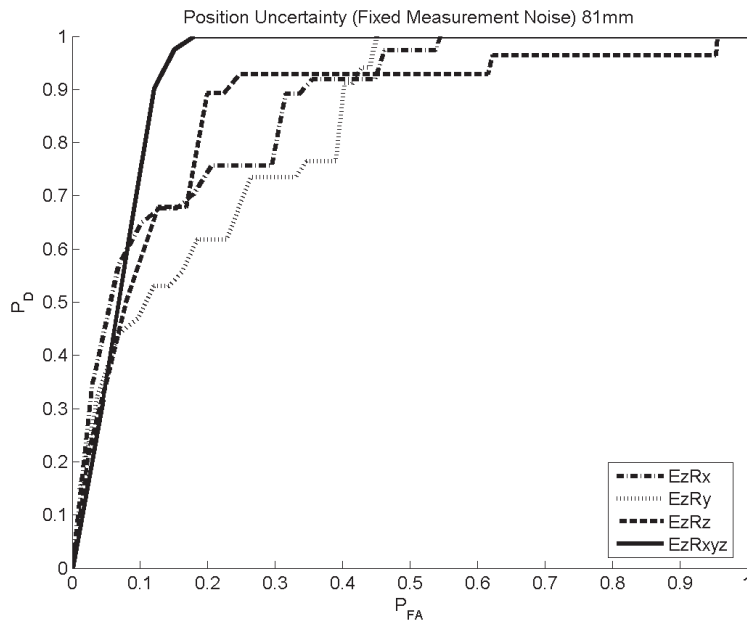


Figure 3: ROC curves plotting probability of detection versus probability of false alarm for the case where measurement noise is included and fixed, but it is assumed that measurement position is uncertain. Single axis and multi-axis results are shown.

In our initial simulations, we consider a system with one transmitter at a fixed orientation and three receiver coils along three perpendicular axes: x , y , and z . We consider a simulated target whose resonant frequencies along horizontal and perpendicular directions are 463 Hz and 168 Hz. These parameters were estimated from 81 mm projectile field data. The target is located 0.5 meters from the sensor. To minimize the effect of the target orientation on conclusions based on this simulation, we use a uniform distribution for the target orientation. Using the dipole model, we calculate the electromagnetic field measured from the target when the receiver coil is located in the three different orientations and add Gaussian noise, as is normally observed from the instrument,

to the simulated field. Using our standard inversion algorithms [2, 9, 10], we obtain the estimated moments, the position and the orientation of the buried target from the simulated noisy field.

One mechanism by which to compare the performance of various system configurations is to consider the mean and standard deviations of the estimated moments/resonant frequencies as a function of the level of the Gaussian noise. Fig. 1 shows the standard deviation data for the simulated 81 mm target. Clearly, the three-axis receive coil provides better performance with increasing noise variance than any of the single axis systems.

In order to further quantify performance gain, the simulated 81 mm projectile was classified against a simulated clutter field where the clutter moments were distributed uniformly. A Bayesian classifier was used to discriminate the UXO object from the clutter using the estimated moments. Testing and training of the classifier were performed separately. Fig. 2 illustrates the classification performance achieved from three single axis and one multi-axis system. Some performance gain is obtained for the three axis system. Fig. 3 illustrates similar results, however in this case we simulated uncertainty in the position of the measurements. In this more realistic case, substantially more performance gain is observed in the case of the multi-axis system.

3. Conclusions

The results presented here indicate that a multi-axis system may potentially provide performance gain for discriminating UXO from clutter. We considered a case of discriminating an 81 mm projectile from a uniform field of clutter in the presence of additive Gaussian sensor noise. When no location uncertainty was included in the problem formulation, performance gains were small for the multi-axis sensor. However, when uncertainty in the exact location of the sensor was incorporated into the simulations, performance gain was enhanced substantially when the multi-axis sensor was utilized. This performance gain is a direct result of more accurate inversions possible with the multi-axis system.

Acknowledgement

This research was supported by the Strategic Environmental Research and Development Program (SERDP) under project UX-1442.

REFERENCES

1. Billings, S. D. and F. Herrmann, "Automatic detection of position and depth of potential UXO using a continuous wavelet transform: SPIE conference on detection and remediation technologies for mines and minelike targets," Orlando, April 21–25, 2003.
2. Collins, L. M., Y. Zhang, J. Li, H. Wang, L. Carin, S. Hart, S. Rose-Pehrsson, H. Nelson, and J. McDonald, "A comparison of the performance of statistical and fuzzy algorithms for unexploded ordnance detection," special issue on Recognition Technology, *IEEE Trans. Fuzzy Systems*, Vol. 9, No. 1, 17–30, 2001.
3. Tatum, S. and L. Collins, "A comparison of algorithms for subsurface object detection and identification using time domain electromagnetic induction data," *IEEE Transactions of Geoscience and Remote Sensing*, Vol. 39, No. 6, 1299–1306, June 2001.
4. Barrow, B. and H. H. Nelson, "Model-based characterization of electromagnetic induction signatures obtained with the MTADS electromagnetic array," *IEEE Transactions of Geoscience and Remote Sensing*, Vol. 39, No. 6, 1279–1285, June 2001.
5. Bell, T. H., B. J. Barrow, and J. T. Miller, "Subsurface discrimination using electromagnetic induction sensors," *IEEE Transactions of Geoscience and Remote Sensing*, Vol. 39, No. 6, 1286–1293, June 2001.
6. Hu, W. and L. M. Collins, "Classification of multiple closely-spaced subsurface objects: application of independent component analysis," submitted to *IEEE Trans. Geosc. Remote Sensing*.
7. Barrow, B. J. and H. H. Nelson, "Model-based characterization of EM induction signatures for UXO/Clutter discrimination using the MTADS platform," UXO Forum, 1999.
8. Carin, L., H.-T. Yu, Y. Dalichaouch, A. R. Perry, P. V. Czipott, and C. E. Baum, "On the wideband EMI response of a rotationally symmetric permeable and conducting target," *IEEE Transactions of Geoscience and Remote Sensing*, Vol. 39, No. 6, 1206–1213, June 2001.
9. Zhang, Y., L. M. Collins, H. Yu, C. Baum, and L. Carin, "Sensing of unexploded ordnance with magnetometer and induction data: theory and signal processing," *IEEE Trans. Geosc. Remote Sensing*, Vol. 41, No. 5, 1005–1015, May, 2003.
10. Y. Zhang, L. M. Collins, and L. Carin, "Model-based statistical signal processing for UXO discrimination: performance results from the JPG-V demonstration," *Detection and Remediation Technologies for Mines and Minelike Targets VII Conference*, International Symposium on Aerospace/Defense Sensing and Controls, Orlando, Florida, April, 2003.